Journal of Anatomy

J. Anat. (2015) **227**, pp474–486 doi: 10.1111/joa.12365

Analysis of human soft palate morphogenesis supports regional regulation of palatal fusion

Adrian Danescu, Melanie Mattson, Carly Dool, Virginia M. Diewert and Joy M. Richman

Faculty of Dentistry, Life Sciences Institute, University of British Columbia, Vancouver, BC, Canada

Abstract

It is essential to complete palate closure at the correct time during fetal development, otherwise a serious malformation, cleft palate, will ensue. The steps in palate formation in humans take place between the 7th and 12th week and consist of outgrowth of palatal shelves from the paired maxillary prominences, reorientation of the shelves from vertical to horizontal, apposition of the medial surfaces, formation of a bilayered seam, degradation of the seam and bridging of mesenchyme. However, in the soft palate, the mechanism of closure is unclear. In previous studies it is possible to find support for both fusion and the alternative mechanism of merging. Here we densely sample the late embryonic-early fetal period between 54 and 74 days post-conception to determine the timing and mechanism of soft palate closure. We found the epithelial seam extends throughout the soft palates of 57-day specimens. Cytokeratin antibody staining detected the medial edge epithelium and distinguished clearly that cells in the midline retained their epithelial character. Compared with the hard palate, the epithelium is more rapidly degraded in the soft palate and only persists in the most posterior regions at 64 days. Our results are consistent with the soft palate following a developmentally more rapid program of fusion than the hard palate. Importantly, the two regions of the palate appear to be independently regulated and have their own internal clocks regulating the timing of seam removal. Considering data from human genetic and mouse studies, distinct anterior-posterior signaling mechanisms are likely to be at play in the human fetal palate.

Key words: aponeurosis; craniofacial; hard palate; medial edge epithelium; palatal shelf; submucous cleft; tensor veli palatini; velopharyngeal.

Introduction

The human face undergoes a major transition from the 4th to the 8th week of embryogenesis. It is during this critical period that genetic and environmental disturbances can lead to serious anomalies of the face, including orofacial clefts. Genetic studies of individuals with clefts and their families have identified many putative genes that could increase the risk of developing a cleft (Jugessur et al. 2009; Leslie & Marazita, 2013). Despite these advances, the mechanism of how the human face forms is relatively poorly understood. This is partially due to a lack of access to human conceptuses at the relevant stages, especially those preserved in a manner suitable for molecular studies.

Facial morphogenesis starts with the migration of neural crest cells that travel from the dorsal margins of the primitive brain to the ventral side (Creuzet et al. 2005). The Hox-negative facial neural crest cells populate the buds that surround the primitive mouth called facial prominences. The neural crest derivatives in the head include intramembranous bones, cartilages, sensory ganglia and connective tissue.

The facial prominences are covered by ectodermally derived epithelium which extends into the oral cavity. The boundary between endodermally and ectodermally derived epithelium is set up by the position of the buccopharyngeal membrane (Waterman, 1977; Kara & Kara, 2007; Verma & Geller, 2009), which breaks down by embryonic day 26 in humans. The boundary between ectoderm and endoderm is not clear because there is no marker that can distinguish these two lineages of epithelium. We can deduce the position of the buccopharyngeal membrane based on case reports where remnants of the membrane were found in the posterior oral cavity (Kara & Kara, 2007; Verma & Geller, 2009). Generally the tags of epithelium lie between the hard and soft palate. Therefore it is likely that endodermal epithelium covers the majority of the soft palate including uvula, tonsillar fauces, the naso and oropharynx.

Correspondence
Joy M. Richman, Faculty of Dentistry, Life Sciences Institute, University of British Columbia, Vancouver, BC, Canada 604 822 3568.
E: richman@dentistry.ubc.ca

Accepted for publication *6 July 2015*
Article published online *24 August 2015*

Initially, individual facial prominences are either delineated by deep grooves or physically separated by epithelium (Abramyan et al. 2015). The medial nasal prominences form the midline of the face (nasal septum, midline of the nose, philtrum, premaxilla and four incisors). The lateral nasal prominences, which are lateral to the nasal pits, form the nasal turbinates and alae of the nose. The maxillary prominences grow extensively to form the majority of the upper jaw, including the upper lip adjacent to the midline, the maxillary and palatine bones. The mandibular prominences form the entire lower jaw. To create a contiguous, smooth appearance of the face, two mechanisms are involved, merging and fusion. Merging is thought to involve differential proliferation and perhaps migration of mesenchyme that together fill out the deep furrows (Pruzansky, 1961; Cox, 2004). Examples of merging in the primary palate are the nasolacrimal groove between the lateral nasal and maxillary prominences, the midline groove between the medial nasal prominences and the midline of the mandibular prominence. Fusion occurs when two epithelial-lined structures come together to create a bilayered epithelial seam that eventually degrades. Following seam removal, mesenchyme from either side penetrates the midline, forming a mesenchymal bridge. Fusion occurs between the medial nasal, maxillary and lateral nasal prominences in most mammals (Jiang et al. 2006; Abramyan et al. 2015). Microforms of cleft lip will occur if the small external grooves are not filled in by merging (Suzuki et al. 2009). In humans, fusion of the lip should be completed by 44 days post-conception and all the grooves should be filled in by 47 days (Ooë, 1981; Diewert, 1983; Kitamura, 1989; Diewert & Shiota, 1990). However, if there is abnormal outgrowth of facial prominences, a cleft lip will occur. The more severe the cleft lip, the more separation of the right and left facial prominences there will be. Thus often cleft lip leads to clefts of the secondary palate (cleft lip with or without cleft palate). CL/P is the most common, non-syndromic orofacial cleft occurring in approximately 1 : 700 births (Dixon et al. 2011; Leslie & Marazita, 2013).

Towards the end of the 6th week the secondary palate begins to develop. The palatal shelves (also called the lateral palatine processes) grow out from the medial sides of the maxillary prominences. The palatal processes assume a vertical position on each side of the tongue but then, during 7th week, horizontal reorientation occurs at the same time as the mandible elongates and the head of the fetus lifts upwards. These movements elevate the maxilla relative to the tongue, clearing the space between the palatal shelves and facilitating their contact (Humphrey, 1969; Diewert, 1983, 1985, 1986). The joined shelves will form a bilayered, medial edge epithelial seam (MEE). The fusion process requires adherence of the two epithelia through cell adhesion and formation of desmosomes (Mogass et al. 2000; Mossey et al. 2009). Growth factors such as transforming growth factor β3 (TGFβ3) mediated by transcription factor IRF6 play an important role in adhesion (Kaartinen et al. 1995, 1997; Proetzel et al. 1995; Miettinen et al. 1999; Cui et al. 2003, 2005; Dudas et al. 2004; Nakajima et al. 2007; Iwata et al. 2013).

There has been much interest in the mode of seam degradation in the secondary palate. There are three processes thought to be involved: apoptosis (Cuervo et al. 2002; Nawshad, 2008), epithelial–mesenchymal transformation (EMT) (Fitchett & Hay, 1989; Martinez-Alvarez et al. 2000; Nawshad, 2008) and migration of the epithelial cells to adjacent epithelia (Cuervo & Covarrubias, 2004; Jin & Ding, 2006; Xu et al. 2006). However, mouse studies in which permanent genetic labels were inserted into the epithelium do not support the idea that EMT occurs *in vivo* (Cuervo & Covarrubias, 2004; Jin & Ding, 2006; Iwata et al. 2014). Regardless of the mode of seam degradation, from a clinical point of view, the failure to remove the epithelium leads to congenital midline cysts of the hard palate (Epstein's pearls) (Kitamura, 1966, 1989; Saunders, 1972) and perhaps submucous clefts.

Palatal shelves additionally fuse with the nasal septum and the primary palate. Unilateral cleft palate may occur when one palatal shelf fails to fuse with the nasal septum. Variants can include fusion with the primary palate but an open palate more posteriorly (Kitamura, 1989; Wyszynski, 2002). The fusion of secondary palate is much slower than the primary palate. Instead of 1 week to form the primary palate, the secondary palate develops from the 7th to the 12th week. Fusion of the hard palate ends by the 8th week and then the soft palate closes by the 10th week. Surprisingly, despite such a long window of susceptibility, isolated clefts of the palate are much less common than cleft lip (1 : 1500) (Mossey et al. 2009). Other differences are that different genes are involved in the two types of clefts (Jugessur et al. 2009; Mossey et al. 2009). Thus it is important from a clinical perspective to screen babies with CPO carefully for other anomalies.

The submucous cleft is a microform of cleft palate and can range from the clinically obvious notching of the hard palate, bifid uvula (Shprintzen et al. 1985a), zona pellucida in the midline, to the absence of a posterior nasal spine, which would only be visible on radiographs (Calnan, 1954; Ha et al. 2013). Furthermore, velopharyngeal insufficiency with no identifiable anatomical defects can occur (occult cleft) (Lewin et al. 1980; Gosain et al. 1999). Generally, velopharyngeal insufficiency is due to an inability of the right and left portions of the levator veli palatini muscle to contact in the midline (diastasis), and thus the soft palate is uncoordinated during speech and swallowing (Kummer et al. 2015). The incomplete development of the midline in submucous clefts could be due to either a failure of fusion or merging.

The prevalence of human submucous clefting in the general population is quite rare (1 : 1200) (Weatherley-White et al. 1972). It is more common to encounter cleft uvula (1 : 100) (Weatherley-White et al. 1972) and the majority of

cases have no other functional defects. However, these prevalence values may be an underestimate due to relatively superficial examination and the exclusion criteria used in previous studies. CPO including clefts of the soft palate is more commonly associated than CL/P with syndromes (Shprintzen et al. 1985b; Mossey & Castilla, 2003; Bell et al. 2013). Detection of a cleft soft palate may trigger further investigations to rule out 22q11.1 deletion or DiGeorge syndrome (OMIM 188400) (Gosain et al. 1999).

The mechanism of soft palate formation is less clear than it might first appear. Several studies on the topic of human palate development were published decades ago (Wood & Kraus, 1962; Kitamura, 1966; Burdi & Faist, 1967; Weatherley-White et al. 1972; Rood, 1973; Poswillo, 1974; Smiley, 1975). There were disagreements as to the mode of closure of the soft palate – some anatomists believed that merging was taking place, whereas others felt that fusion was the primary mechanism. In one of the former studies (Burdi & Faist, 1967) 31 embryos and fetuses, ranging in age from 7 to 12 weeks and in size from 18 to 75 mm crown–rump length, were examined in serial sections. These authors proposed that two mesenchymal growth centers at the posterior edge of the newly fused hard palate extend outward without forming a seam. While it seemed that the study contained a large sample, there were in fact just two specimens that were of an appropriate age. Other prominent embryologists cited the Burdi & Faist (1967) study, which spread the concept of merging in the soft palate to a wider audience (O'Rahilly & Muller, 2001; Wyszynski, 2002; Sperber & Guttman, 2010). Fusion was described in the soft palate in two studies that also had low numbers of fetuses (Kitamura, 1966; Smiley, 1975). A hybrid mechanism was also proposed whereby fusion occurs in the anterior two-thirds of the soft palate while the posterior third develops by merging (Poswillo, 1974).

The clinical evidence that supports fusion includes the presence of epithelial cysts in the soft palate. The prevalence of midline palatal cysts or Epstein's pearls is high in the hard palate (54% of newborns (Monteagudo et al. 2012) but much rarer in the soft palate (Caylakli et al. 2005; Tsai et al. 2013). A Japanese study found epithelial cysts in the midline of the soft palate in the early fetal period (53–55 days post-conception; (Kitamura, 1966), so perhaps many of these resolve prior to birth.

The goal of our study is to densely sample the 54- to 74-day human fetus, paying close attention to the period around 60 days' gestation, in order to determine (i) the timing of hard palate seam removal and (ii) the presence or absence of a midline seam in the soft palate. From the specimens examined we have determined that fusion occurs in both regions of the palate but that the rate of epithelial seam removal in the hard palate is much slower than in the soft palate. In addition, the thickness and organization of the medial edge epithelia were different in the two regions, although keratin expression was similar.

Methods

Preparation of specimens and processing into paraffin

Human conceptuses of European descent originated from elective terminations carried out at the University of Washington between 1988 and 1991. The pathologist examined each fetus and determined that they were normal based on external appearance and the health history of the mother. However, at the time it was not the practice to screen externally normal conceptuses for chromosomal anomalies. All fetuses were staged at the time of termination using a combination of crown–rump and foot length (Supporting Information Fig. S1). The ages ranged from 53 to 74 days post-conception, therefore all specimens were past stage 23 of the Carnegie embryo staging system. For this reason, we refer to days post-conception rather than stages. The typical condition was a partial head, lacking the occipital region, brain and sometimes mandible. Some of the specimens were sectioned at that time and others were maintained for several years as wet specimens until the present study was initiated. Wet specimens were decalcified with 7% EDTA for at least 8 weeks, washed in phosphate-buffered saline (PBS), dehydrated through an ethanol series and then processed into paraffin. Specimens were sectioned in the transverse/coronal or horizontal plane at a thickness of 7 μm. This study was approved under UBC Human Ethics protocol #H08-02576.

Histochemical and immunohistochemical staining procedures

Newly created sections and archival slides that were unstained, were stained with Picrosirius red/Alcian blue or Hematoxylin/Eosin. Staining with Picrosirius red/Alcian blue consisted of sequential immersion in 1% Alcian blue in acetic acid for 30 min, 1% acetic acid for 5 min, water for 5 min, Picrosirius red for 1 h in the dark, followed by 1% acetic acid for 5 min and water for 5 min. For H/E slides, Shandon hematoxylin (Thermo Scientific) was diluted 50% in water, slides were immersed for 2 min, rinsed in tap water for 5 min, immersed in saturated lithium carbonate solution for 1 min, dipped in 1% Eosin Y 30 times, and rinsed in water for 5 min. Stained slides were dehydrated through an ethanol series and coverslipped.

For immunohistochemistry (IHC) MF20 mouse monoclonal supernatant (Developmental Studies Hybridoma bank) was added neat or mouse anti-cytokeratin (Z0622; Dako) was used at a dilution of 1 : 1000. This pan-cytokeratin antibody cross-reacted with keratins uniquely expressed in mucosal epithelium such as K4, 13 and 19 as well as keratins that are found throughout the keratinized and non-keratinized oral mucosa, including K5, 6 and 16 (Presland & Dale, 2000). Pretreatment for MF20 consisted of Proteinase K (5 $\mu g\ mL^{-1}$) for 10 min at 37 °C. For anti-cytokeratin, sections were steamed in a DIVA Decloaker (Biocare Medical) for 20 min. The Vector ABC Kit was used according to the manufacturer's instructions (Vector Labs, Canada) using diaminobenzidine-peroxide detection. When detection was completed, slides were counterstained with hematoxylin for 30 s. Note we removed coverslips from some previously stained slides by soaking them for several days in xylene. Some of these archival sections were successfully used for immunohistochemistry.

3D reconstruction of human fetuses at various stages of palatogenesis

Eleven sectioned and stained human specimens between 54 and 64 days of development were photographed serially at the hard-soft

palate junction on a Zeiss Axiophot compound microscope. The images were imported in to WinSurf 3D Reconstruction program (SURFdriver Software, Kailua, HI, USA, developed by S. Lozanoff). The structures of interest were traced and converted to a stack. The areas traced included the hard palate, soft palate, palatine bones, midline epithelial seam, palatine aponeurosis, and the nasal septum. The stacks were aligned within the WinSurf program and smoothed to create a representation of the hard-soft palate junction. Screen captures were created from different views of the reconstruction and imported into Adobe Photoshop.

Results

In terms of general development, the conceptuses used in the present study were in the early fetal period or the start of the second trimester. The earliest bones to ossify were the mandibular (dentary), palatine process of the maxillary bone, maxillary, vomer and the transverse portion of the frontal bone making up the superior orbital wall. By 70 days the majority of the facial bones were present. The primary dentition was in the bud stage in the 54-day specimens. By 74 days all teeth in the deciduous dentition had initiated and were in the cap or bell stage. The youngest fetuses in the sample had complete fusion of the primary palate and secondary palate was beginning to close. The tongue was fully formed and the hyoglossus and genioglossus muscle layers had become well organized. The shelves of the palate were reoriented horizontally in all specimens. The hard palate was fused in all specimens except for one 54-day conceptus (Table 1). The soft palate condition ranged from fully open to closed, thus the sample covered the relevant period of development (Table 1).

It was important to determine anatomical landmarks to identify the different regions of the hard and soft palate that could be recognized even if the plane of section varied. The junction between the hard and soft palate was identified by (i) the change in orientation of the palatal nerve from vertical to a horizontal position as it enters the soft palate, (ii) the presence or absence of primary molar tooth germs and (iii) the presence or absence of the horizontal palatine process of the palatine bones. The aponeurosis was the main marker for the middle soft palate and is a tendon-like structure into which the palatal musculature inserts (De la Cuadra Blanco et al. 2012). We defined three soft palate subregions: anterior to the aponeurosis, within the aponeurosis and posterior to the aponeurosis. The posterior soft palate included the tensor veli palatini muscle and uvula.

The soft palate is not closed at 54 days post-conception

We began our analysis at 54 days because the 53-day specimens (n = 3) had incomplete closure of the hard palate and the soft palate was completely open (data not shown). In the five 54-day fetuses, all except one still had a robust MEE in the hard palate (Tables 1 and 2A,B, Fig. 1A,A′). In the anterior soft palate, three of the five specimens had not yet closed; the other two had closed anteriorly and had a midline seam (Fig. 1B,C′; Tables 1 and 2B). There was only one 54-day specimen that had midline contact in the middle and posterior palate with a seam present throughout (Fig. 1B–E′). The midline epithelium in the soft palate was thicker and more irregular than in the hard palate (Fig. 1B′, C′D′; Supporting Information Fig. S2C′–C″). We tested the pan cytokeratin antibody on the one 54-day specimen that had the midline seam. Archival sections from which the coverslips were removed were stained with pan-cytokeratin antibody to assess whether epithelial–mesenchymal

Table 1 Characteristics of palate closure in 54- to 74-day fetuses.

Days post-conception	Hard palate	Soft palate		
		Anterior	Middle	Posterior
54 day-1	S	S	S	S
54 day-2	S	O	O	O
54 day-3	S	O	O	O
54 day-4	S	S	O	O
54 day-5[1]	O	O	O	O
57 days-1	S	O	O	O
57 days-2	S	S	S,A	S,A
57 days-3[2]	S	O	O,A	O
57 days-4	MB,R	MB,R	MB,R,A	MB,R
57 days-5[3]	S	O	O	O
57 days-6	S	MB,R	MB,R,A	O
57 days-7	S	MB,R	MB,R,A	O
57 days-8[4]	S	S	O	O
57 days-9	S	MB,R	S,A	S (posterior tip open)
57 days-10	S	MB	MB,A	O
57 days-11	S	S	O	O
57 days-12	S	MB,R	S,A	S (posterior tip open)
59 days-1	MB	MB	MB,A	No data
59 days-2	S	S	No data	No data
64 days-1	MB	MB,R	MB,R,A	MB
64 days-2	MB,R	MB	MB,A	S
64 days-3	MB,R	No data	No data	No data
67 days-1	MB,R	MB	MB,A	S
67 days-2	MB,R	MB	MB,A	No data
67 days-3	MB,R	MB	MB,A	0
70 days-1	MB,R	MB	MB,A	MB
70 days-2	MB,R	MB,R	No data	No data
74 days-1[5]	MB,R	MB	MB,A	MB

A, aponeurosis; MB, mesenchymal bridge; O, open, no contact; R, epithelial remnants in midline; S, medial edge seam.
[1]Medial surfaces of soft palate right shelf have no MEE epithelium due to tearing of tissue.
[2]Medial surfaces of soft palate shelves have no MEE epithelium due to tearing of tissue.
[3]Sections are horizontal and tilted.
[4]Medial surfaces of posterior soft palate have no MEE epithelium due to tearing of tissue.
[5]Sections are horizontal.

Table 2 Seam presence or absence in the hard (A) and soft (B) palate.

Specimen	Seam	Epithelial remnants	No seam or epithelial remnants in midline
(A) Hard palate			
54 days (n = 5) 1/5 not fused	4	0	0
57 days (n = 12)	11	1	0
59 days (n = 2)	1	0	1
64 days (n = 3)	0	2	1
67 days (n = 3)	0	3	0
70 days (n = 2)	0	2	0
74 days (n = 1)	0	1	0

	Anterior		Middle		Posterior
Days post-conception	Contacting with seam	Mesenchymal bridge with epithelial remnants	Contacting with seam	Mesenchymal bridge with epithelial rudiments	Contacting with seam or remnants
(B) Soft palate					
54 days (n = 2)[1]	2/2	0	1/2	0	1/2
57 days (n = 9)[2]	3/9	5/9	3/8	3/8	4/4
64 days (n = 2)[3]	0	1	0	1	1/1
67 days (n = 3)[4]	0	0	0	0	0/2
70–74 days (n = 3)[5]	0	1/3	0/2	0/2	0/2

[1]Medial surfaces of soft palate right shelve have no MEE epithelium due to tearing of tissue.
[2]Medial surfaces of soft palate shelves have no MEE epithelium due to tearing of tissue.
[3]Sections are horizontal and tilted.
[4]Medial surfaces of posterior soft palate have no MEE epithelium due to tearing of tissue.
[5]Sections are horizontal.

transformation was taking place. Specific staining was observed in the endodermally derived soft palate, tongue and pharyngeal epithelium (Fig. 1C′,E′). The midline seam was also positive for cytokeratin (Fig. 1C′,E′). The weak staining was likely due to retention of the previous histochemical stain rather than EMT. The condensations for the developing palatine aponeurosis were present lateral to the midline (Figs 1B and S2C). The posterior soft palate exhibited horizontal shelves that were either in light contact (Fig. 1D,D′,E,E′) or open (Fig. S2C,C′).

A medial epithelial seam is present in the soft palate and then rapidly degraded

Twelve 57-day specimens were examined. All of these conceptuses had completed hard palate fusion. The MEE seam was present in all sections through the hard palate (Figs 2A–A′ and 3A,B′, E,F″), especially on the oral side (Tables 1 and 2A, Fig. 3A,B′, Supporting Information Fig. S3A,A′). There was more variability in the status of the anterior soft palate (Tables 1 and 2B), ranging from being open (n = 3/12) to fused with a seam anteriorly (n = 4/12; Fig. S3B,B′) and fused with epithelial remnants (n = 5/12, Figs 2B,C′ and 3D,D′,G,G′). Several specimens originally fixed in Carnoy's solution and that were not previously stained, worked well in immunohistochemistry staining. Cytokeratin antibody staining was strong in all areas of the oral cavity (Figs 2C,C′E,E′ and 3D,D′,G,G′). Positively stained endodermal epithelium was found on the dorsum of the tongue, lining the pharynx and Eustachian tube. In addition there was staining for cytokeratin in the midline epithelial seam and remnants of the middle and posterior soft palate (Figs 2C′ and 3D′,G′). The aponeurosis condensation was present in the mid-soft palate (n = 5/12; Figs 3C,D,H,H′ and Fig. S3C,C′). The MF-20 antibody confirmed the presence of the levator veli palatini and distinguished the myoblasts from the fibroblasts comprising the aponeurosis (Fig. 2F,F′). The posterior soft palate was open in eight of the 57-day specimens (8/12; Table 1; Figs 2D–F′ and 3I,I′). In the remaining four specimens where posterior contact was achieved, a seam was present between the palatal shelves (Figs 3D,D′ and S3D,D′; Tables 1 and 2B). The presence of a seam extending all the way into the most posterior extension of the soft palate is consistent with fusion being the mechanism of closure rather than merging.

Between 59 and 74 days the mesenchyme was continuous across the midline of the hard and soft palates in all but one specimen. A 64-day specimen had a seam in the posterior soft palate (Fig. 4C,C′). The more typical absence

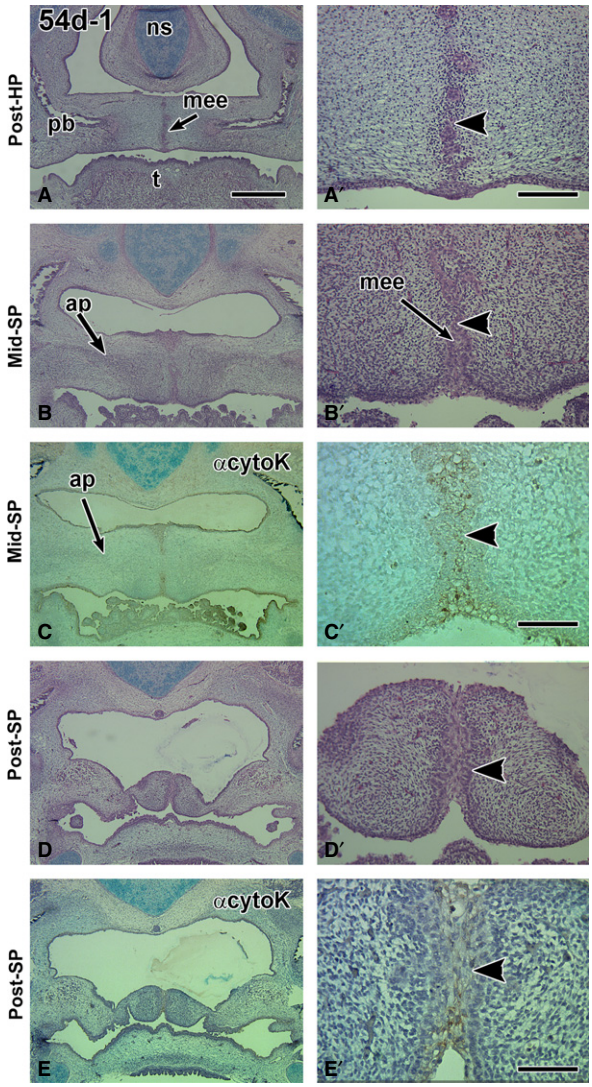

Fig. 1 Frontal sections through a 54-day fetus displaying a degrading seam in the hard palate and a multilayered medial edge epithelial seam in the soft palate. (A,A′) The posterior boundary of the hard palate is distinguished by the medial processes of the palatine bones. A fragmenting medial edge epithelial seam is present (arrowhead). (B, B′) The middle soft palate is identified by the presence of the aponeurosis and absence of palatine bone. A medial epithelial seam appears to be present but is hard to distinguish with H & E staining (arrowhead). (C,C′) The coverslip was removed on an adjacent slide to (B) and stained with pan-cytokeratin antibody. The antibody distinguishes epithelium (arrowhead) from mesenchyme. All epidermal and endodermal (posterior tongue, oropharynx) epithelia are stained with the antibody. (D,D′) The posterior soft palate has a very thick medial seam that is stained weakly with pan-cytokeratin antibody (arrowhead). Ap, aponeurosis; ns, nasal septum; pb, palatine bone; t, tongue. Scale bars: (A) 1 mm, (A′) 200 μm and applies to B′ and D′, (C′,E′) 100 μm.

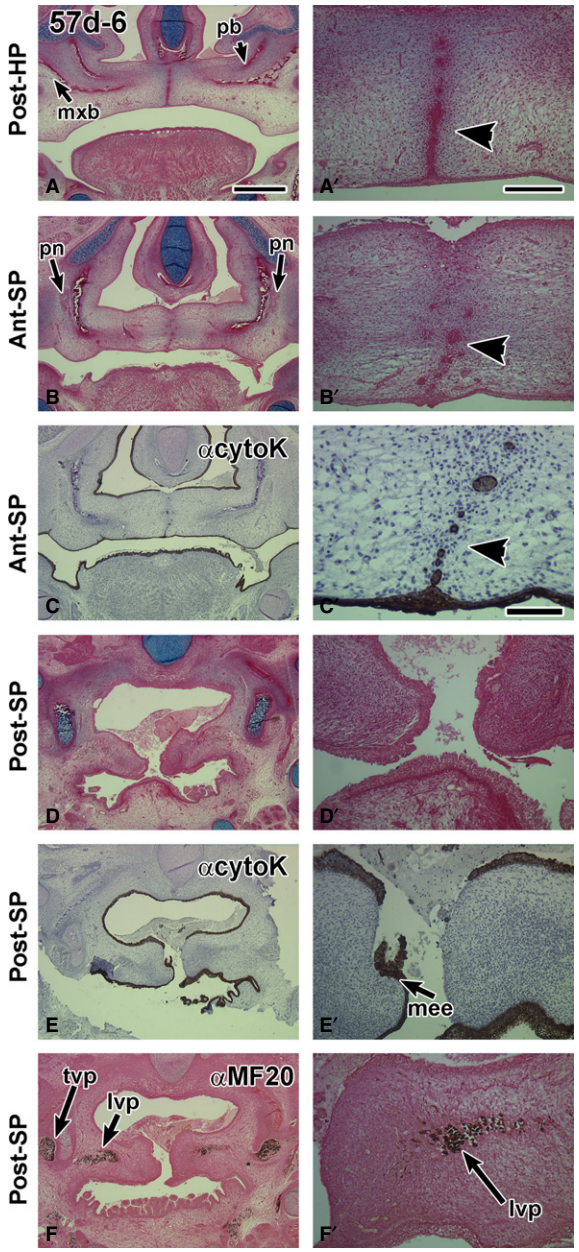

Fig. 2 Frontal sections through a 57-day fetus with a midline epithelial seam in the hard palate while in the soft palate the seam is degrading. (A,A′) A robust medial edge seam in the hard palate that is intact orally (arrowhead) and breaking down nasally. (B,B′) The border with the soft palate is identified by the presence of the palatine nerve lateral to the palatine bones. The midline appears to have epithelial islands (arrowhead). (C,C′) The pan-cytokeratin antibody identifies clearly that there are epithelial remnants in the midline (arrowhead in C′). The antibody also stains the dorsum of the tongue and pharynx. (D,D′) A posterior section through the open soft palate. (E,E′) an adjacent section to (D) stained with anti-cytokeratin. The medial edge epithelium is torn, which is an artifact of specimen preparation. (F,F′) Myosin heavy chain antibody MF-20 stains the palate musculature. lvp, levator veli palatini; mee, medial edge epithelium; mxb, maxillary bone; pb, palatine bone; pn, palatine nerve; t, tongue; tvp, tensor veli palatini. Scale bars: (A) 1 mm, (A′) 200 μm and applies to B′,D′,E′,F′; (C′) 100 μm.

of epithelium in the midline of the soft palate was confirmed by the lack of epithelial remnants in a 67-day specimen stained for cytokeratin (Supporting Information Fig. S4C,C′). The presence of organized musculature in the soft palate was observed at 67 days (Fig. S4D,D′). Based

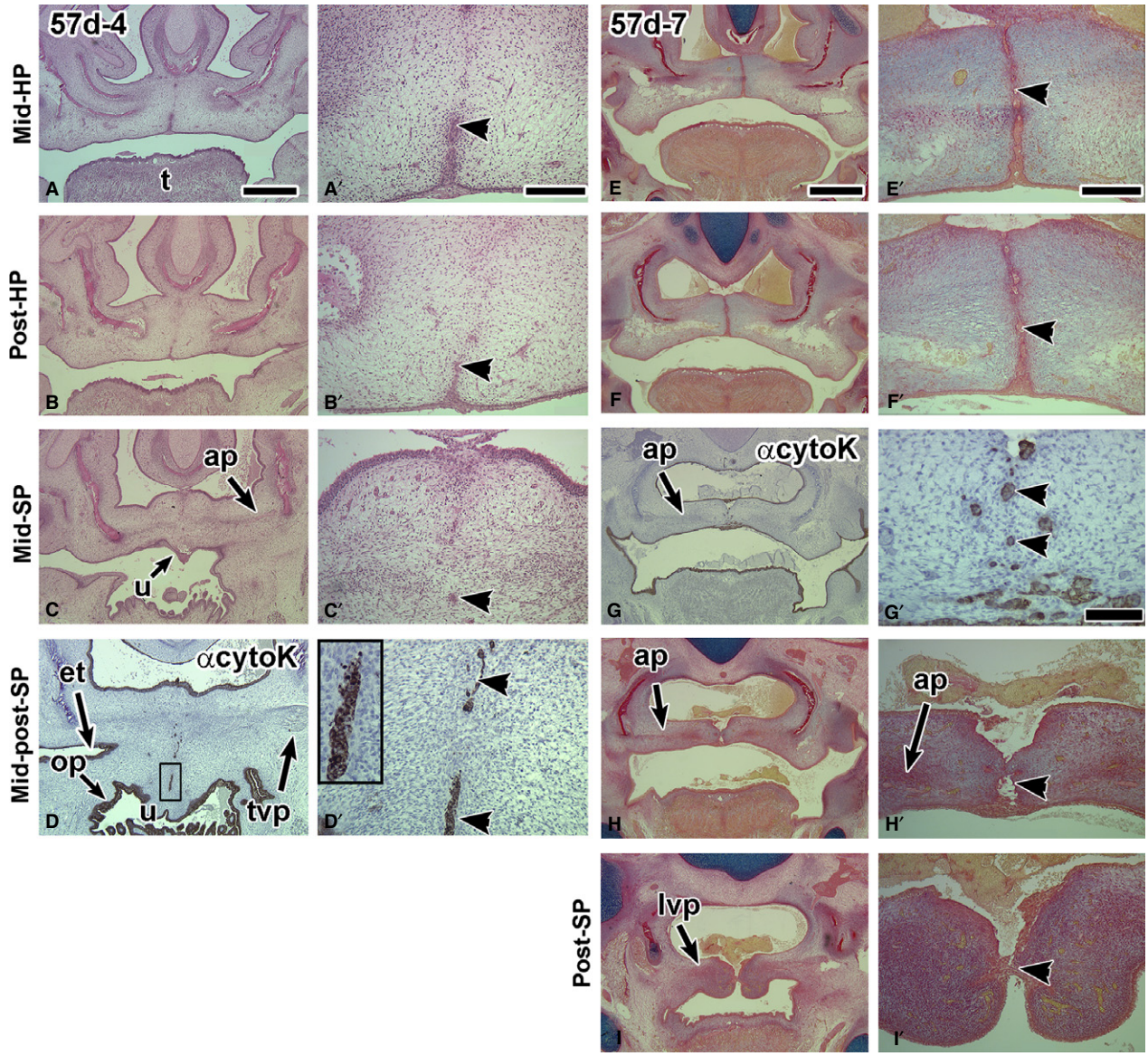

Fig. 3 Sections through two 57-day fetuses contrasting the longevity of the hard palate midline epithelial seam and the rapidly degrading seam in the soft palate. The specimen in A–D′ is tilted so that the left side is cut more posteriorly than the right side. (A,B′) The hard palate retains the midline epithelial seam on the oral side of the palate (arrowheads). (C,C′) In contrast, the soft palate has no seam anteriorly (right side of images in B,C). A possible epithelial remnant is present in the mid soft palate (C′). (D,D′) More posteriorly, numerous epithelial remnants remain in the midline of the soft palate. The anti-cytokeratin antibody stains all epithelia including non-cornified, endodermally derived mucosa lining the Eustachian tube and pharynx. (E–I′) Another example of a 57-day conceptus sectioned frontally. (E,F′) A bilayered epithelial seam in the hard palate is present together with a degrading seam in the middle soft palate (G-G′). (H,H′) The middle soft palate is partially fused and the posterior soft palatal shelves are barely adhering (I,I′). et, Eustachian tube; t, tongue. Scale bars: (A) 1 mm, (A′) 200 μm and applies to all high-power views; (E) 1 mm; (E′) 200 μm and applies to all high power views except G′; (G′) 100 μm.

on our study, it is likely that a seam had formed in the soft palate at around 57 days but was rapidly degraded prior to 64 days.

3D reconstruction of the medial epithelial seam and surrounding structures in the hard and soft palate

To clarify the relationship of a seam to the soft and hard palate we reconstructed a variety of specimens ranging in age from 54 to 74 days (54 days $n = 2$, 57 days $n = 4$, 59 days $n = 2$, 64 days $n = 1$, 67 days $n = 1$, 70 days $n = 1$, 74 days $n = 1$). In the 54-day specimen, a midline seam was present in the anterior soft palate (Fig. 5A,B). Posteriorly, the shelves were open, relatively short, and had a rounder shape than the actively fusing parts of the shelf. These dome-shaped shelves appeared tethered to the lateral pharyngeal wall. A midline epithelial seam was also present throughout the hard palate and into the soft palate in the

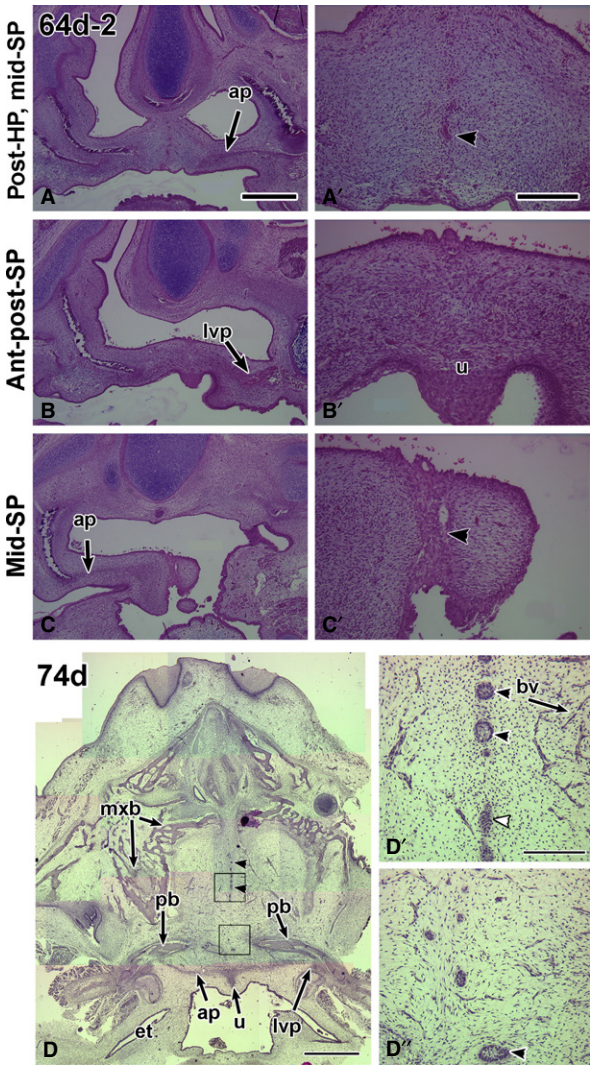

Fig. 4 Fusion of the hard and soft palate in 64- and 74-day specimens. (A,A′) The specimen is tilted towards the left side and therefore the right palate is cut at a more anterior plane than the left palate. Very few epithelial remnants remain in the hard palate (arrowhead in A′). (B,B′) The anterior and posterior soft palate have completely fused. In the midline, the uvula is present and is covered by a very thick layer of epithelium (B′). (C,C′) The right side of the palate is cut through the aponeurosis, and the left side through the posterior soft palate. The midline epithelial seam is present in the posterior part of the section (C′). (D,D″) Horizontal section through a 74-day specimen. The section passes through the full hard palate as well as the three regions of the soft palate as defined in this study, anterior to the aponeurosis, within the aponeurosis and posterior to the aponeurosis. Midline epithelial remnants are present in the hard palate (arrowheads in D). (D′,D″) High-power views of the epithelial remnants and micro-vasculature in the hard palate. ap, aponeurosis; bv, blood vessel; et, Eustacian tube; lvp, levator veli palatini; mxb, maxillary bone; pb, palatine bone; u, uvula. Scale bars: (A) 1 mm, (A′) 200 μm and applies to all high-power views; (D) 2 mm, (D′,D″) 200 μm.

57-day specimens (Fig. 5C,D). The terminal portions of the soft palate shelves transitioned to a thin and tapered shape as they elongated toward the midline (Fig. 5C,D). By the

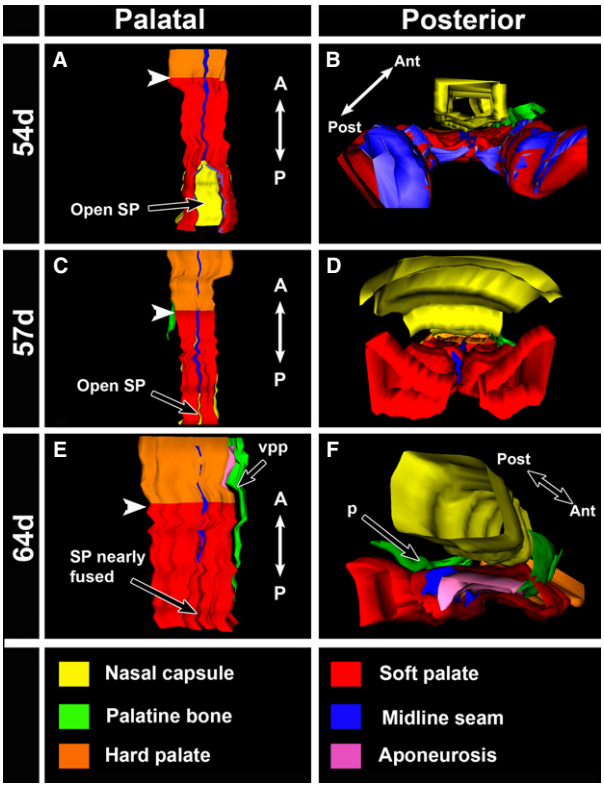

Fig. 5 Reconstructions of segmented regions using WinSurf software. Screenshots were captured from a palatal and a posterior view. White arrowheads point to the hard palate–soft palate junction. In the 54-day specimen (A,B), the seam is present through the portion of the soft palate that is fused. The unfused soft palate shelves are significantly smaller in volume than the fused shelves, indicating that growth still needs to occur to promote contact. The dome shape of the unfused shelves can be clearly seen in the posterior view (B). In the 57-day specimen (C,D), the midline seam is present in both the hard and soft palate. The unfused shelves in this specimen are larger in volume and closer to contacting in the midline than the shelves of the 54-day specimen. The 57-day shelves have a different shape and are trapezoidal in appearance. (E,F) In the 64-day specimen the seam in the hard palate is still present but in the anterior soft palate there is a gap where the seam has degraded. The seam then reappears in the middle to posterior fusing soft palate. The narrow band that is the aponeurosis (purple) can also be seen in to the left palatal shelf (F). SP, soft palate; vpp, vertical plate of the palatine bone.

64th day, the medial epithelial seam (Fig. 5E,F) had partially degraded and the aponeurosis approached the midline.

Discussion

Based on the presence of a midline seam or remnants thereof in the most posterior extent of the soft palate, we conclude that fusion is the primary mechanism of closure. The alternative hypothesis of fusion followed by a period of merging was not supported. If a dual-mechanism was being employed, we should have found specimens with a seam in the anterior-mid soft palate and no seam posteriorly. Even though the midline epithelial seam is more rapidly

degraded than in the hard palate, we sampled enough embryos that had apposed palatal shelves in the posterior palate to see a seam. It is the differential rate of seam removal in the hard and soft palate combined with natural variation in development of human fetuses that accounts for the differences in previous palate literature.

Differences in the maturation clock for the hard and soft palate correlate with differences in gene expression

In our study we have in essence shown there are separate developmental clocks that operate in the anterior and posterior palates (Fig. 6A–C). In the anterior hard palate, the rate of contact of the palatal shelves is fairly rapid, between 44 and 54 days, but the degradation of the MEE is very slow, taking another 20 days or more. Indeed, remnants of the midline seam are found all the way up to birth (Fig. 6C) (Kitamura, 1966, 1989). The contrast in timing is exemplified by the persistent seam in the hard palate, juxtaposed with the fused anterior and middle soft palate, already bridged by the palatine aponeurosis in 57-day specimens (Fig. 6C). Other differences between the hard and soft palate are that instead of two tightly organized layers of epithelium in the hard palate, in the soft palate the epithelium is multilayered (Fig. 6C). We also noted that the epithelium was frequently thin or torn in the open posterior soft palate.

It is likely that the differences in epithelial–mesenchymal interactions in the two regions of the palate are affected by well-documented differences in gene activity in the posterior vs. anterior palatal shelves. For example, in the mouse, the anterior palate expressed higher levels of ligands *Fgf10, Wnt5a* and *Bmp4* as well as transcription factors *Shox2* and *Msx1* (Bush & Jiang, 2012; Smith et al. 2012). In the posterior palate few ligands have been identified yet; however, transcription factors *Tbx22, Mn1, Meox, Barx1* are all strongly expressed posteriorly (Bush & Jiang, 2012; Smith et al. 2012). Recently, a genome-wide profiling experiment was carried out on the anterior and posterior post-fusion palates of E15.5 mice (Iwata et al. 2014) (GEO accession number GSE46211). A full analysis has not yet been published but using GEO2R, the top 250 with the greatest fold expression differences include most of the genes mentioned above. There are hundreds of other genes that are also differentially expressed anterior and posterior to the first molar tooth bud, including many in the TGFβ signalling pathway.

Clefting phenotypes support the concept of independence of the anterior (hard) and posterior (soft) palates. In some mouse models, it has been shown that the posterior

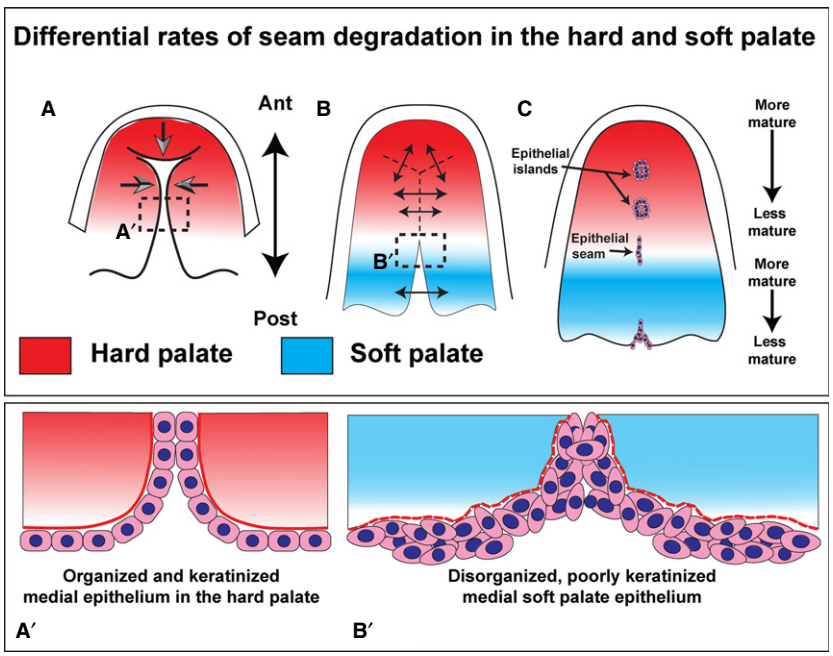

Fig. 6 An update of the diagram included in the 1967 study on palatal morphogenesis by Burdi & Faist (1967). Hard palate development is unchanged from the previous published diagram with the palatal shelves growing towards the midline and primary palate. Modifications include the addition of gradients to indicate the maturity of the seam. The rate of maturation of the seam in the hard and soft palates occurs independently in each region. The soft palate seam may be completely removed at the same time as there is a seam present in the posterior hard palate. (A) Contact occurs and the shelves fuse in an anterior-posterior direction (B). As the hard palate is fusing, the soft palate shelves grow outwards from the lateral pharyngeal wall and contact in the midline (B), after which point fusion occurs and the midline epithelial seam is degraded (C). The inserts show the differences in the appearance of the hard vs. soft palate epithelium at the point of fusion. The hard palate epithelium (A′) is highly organized and forms a clear bilayer. The soft palate epithelium (B′), even at the medial surfaces, is disorganized and bulky, with clumping of cells. Both types of ectoderm and endodermal epithelia are keratinized, as shown by the pan-cytokeratin antibody used in the present study.

palate can fuse successfully even though the anterior palate is cleft due to a failure of fusion with the primary palate (Hilliard et al. 2005; Yu et al. 2005; Gu et al. 2008). A similar hard palate cleft with a fused soft palate has also been produced by teratogenic exposure in rats (Schupbach, 1983). Differences in molecular profiles of the hard and soft palate likely exist in humans and could lead to regional differences in epithelial–mesenchymal interactions.

Conservation of soft palate fusion across Mammalia

Comparative work between extant groups of mammals offers insights into the predominant mode of soft palate closure and perhaps also into the evolution of palate morphogenesis. In the mouse it is well known that the soft palate develops by fusion, not merging (Walker & Fraser, 1956; Smiley & Koch, 1972; Smiley, 1975; Xu et al. 2006). In the Syrian hamster, the soft palate also formed an epithelial seam that was removed by apoptosis, exfoliation and migration of epithelial cells (Shah & Chaudhry, 1974). In the rat there is a seam in the soft palate (Coleman, 1965; Schupbach, 1983). After fusion and mesenchymal bridging, there is a groove on the oral side of the palate that is filled in by merging, similar to merging in the primary palate (DeAngelis & Nalbandian, 1968). A single study has been performed on non-human primates. In that study, 37 baboon embryos were analyzed between 30 and 64 days (estimated) post-conception (Bollert & Hendrickx, 1971). In the 53-day and older specimens, the soft palates were formed with the exception of the uvula, which was still not formed in the oldest 64-day specimens. Upon inspection of these specimens, no epithelial remnants were seen in the soft palate, so the authors concluded that the soft palate must have formed by merging. We would reinterpret the presence of epithelial islands to indicate that fusion has taken place. As fusion appears to be the only mode of palate closure in extant mammals, the most parsimonious view is that fusion was also the primary mechanism in extinct mammals. Taking a larger view of all amniotes, the reptilian line has many variants on palate morphology ranging from naturally cleft to fused (Abramyan et al. 2014). There is only one taxa, the crocodilians, in which the secondary palate undergoes fusion (Ferguson, 1981). It is unclear whether the steps of fusion are indeed similar to mammals; however, it appears that palatal fusion has evolved separately in crocodilians.

Mouse and human genetics identify candidate signaling pathways involved in soft palate fusion

There are hundreds of mouse models with complete cleft secondary palate (Gritli-Linde, 2007; Bush & Jiang, 2012) but only a handful of these develop a microform of clefting specifically affecting the soft palate. The TGFβ signaling pathway is the most frequently associated with soft palate or submucous clefts. *Tgfβ3* null mouse mutants all exhibit some degree of clefting of the palate (Kaartinen et al. 1995, 1997; Proetzel et al. 1995) depending on the background (Iwata et al. 2014). On a C57BL/6 background, 50% of the fetuses have partial clefts affecting mainly the soft palate (Cui et al. 2005). Epithelial deletion of one of the receptors for TGFβ3, *Tgfbr2*, generated submucous clefts in 100% of the offspring as well as occasional cleft soft palate (Xu et al. 2006). The midline epithelium was retained in the soft palate in these animals due to lack of apoptosis and excessive proliferation. Recently, the same epithelial deletion of *Tgfbr2* was analyzed again and this time the mesenchymal changes were studied (Iwata et al. 2014). The upregulation of Wingless-related antagonists, Dkk1 (Dikkopf) and 4, reduced the levels of Wnt signaling in the mesenchyme, leading to decreased muscle mass in the soft palate. While it is impossible to rule out a contribution of the cleft itself to the decreased muscle volume, there are also structural changes in the organization of muscle fibers. Thus from the mouse data at least the TGFβ and Wnt signaling pathways have specific roles in soft palate morphogenesis.

There are two human syndromes in which soft palate clefts with or without submucous clefting of the hard palate are exhibited. In Loeys-Dietz syndrome (OMIM 609192) (Loeys et al. 2005; Van Laer et al. 2014) there are loss-of-function mutations in *TGFBR1,TGBR2, TGFB2* or *SMAD3* (Cardoso et al. 2012) and the clinical features commonly include clefts of the soft palate and more specifically cleft uvula. Therefore, TGFβ signaling is very likely regulates normal soft palate fusion in humans, perhaps by regulating adhesion of the shelves.

Mutations in the T-box transcription factor *TBX22* cause X-linked cleft palate with or without ankyloglossia (OMIM 303400). The cleft phenotypes include submucous cleft, cleft soft palate, velopharyngeal insufficiency and/or cleft uvula (Lowry, 1970, 1971; Braybrook et al. 2001). *TBX22* variants are also associated with increased risk of isolated or non-syndromic cleft palate (Marcano et al. 2004; Suphapeetiporn et al. 2007). The mouse *Tbx22* germline knockout closely mirrors the human syndrome and affects mainly the soft palate (Pauws et al. 2009).

In addition to the aforementioned syndromes, several deletions affecting chromosome 22 lead to soft palate clefts. Microdeletions of chromosome 22q12 cause cleft soft palate (Davidson et al. 2012; Beck et al. 2015; Breckpot et al. 2015). The candidate gene in this location that is associated with palate development is the transcription factor MN1. Mouse studies indicated that *Mn1* is expressed in the posterior palate and lies upstream of *Tbx22* (Liu et al. 2008). Furthermore, the germline knockout of *Mn1* causes a similar phenotype to the *Tbx22* deletion, incomplete cleft palate (Meester-Smoor et al. 2005). The microdeletion of 22q11.1 causes DiGeorge syndrome and the T-box gene, *TBX1*, is within the critical region (Papangeli & Scambler, 2013). The constellation of palate phenotypes includes

velopharyngeal insufficiency, submucous clefts and cleft palate. The *Tbx1*$^{-/-}$ mouse mirrors most of the human phenotypes, including complete clefts (41%), anterior clefts (47%), soft palate clefts (12%) and cardiac defects (Jerome & Papaioannou, 2001; Funato et al. 2012). Thus although many genes are deleted in the same region as *TBX1*, the top candidate for causing the craniofacial and pharyngeal pouch phenotypes is *TBX1*.

In conclusion, our work is significant in terms of understanding the human abnormalities of the soft palate. Seam degradation normally occurs quickly but we can speculate that any delay in the removal of the seam would interfere with midline insertion of the levator veli palatini into the aponeurosis. The disturbance of muscle morphogenesis in the soft palate could be linked to hypernasal speech (Ruda et al. 2012; Kummer et al. 2015), velopharyngeal insufficiency and submucous clefting. In addition, the presence of a seam leads to the possibility that retained epithelial islands could form cysts in the soft palate. From the literature we surmise this is a much rarer complication than microforms of cleft palate. Our work may also assist in the understanding of velopharyngeal insufficiency not associated with clefting as well as hypernasal speech abnormalities, both of which could be due to abnormal fusion of the soft palate. Time will tell whether some of these other soft palate abnormalities will be included as microforms of cleft palate.

Acknowledgements

This work formed part of the requirements for MSc theses for M.M. and C.D. The work was supported by Faculty of Dentistry, University of British Columbia research funds to J.M.R. and by previous BC Health Care Research Foundation grants to V.M.D.

Conflict of interest

The authors declare there are no conflicts of interest.

References

Abramyan J, Leung KJ, Richman JM (2014) Divergent palate morphology in turtles and birds correlates with differences in proliferation and BMP2 expression during embryonic development. *J Exp Zool B Mol Dev Evol* **322**, 73–85.

Abramyan J, Thivichon-Prince B, Richman JM (2015) Diversity in primary palate ontogeny of amniotes revealed with 3D imaging. *J Anat* **226**, 420–433.

Beck M, Peterson JF, McConnell J, et al. (2015) Craniofacial abnormalities and developmental delay in two families with overlapping 22q12.1 microdeletions involving the MN1 gene. *Am J Med Genet A* **167**, 1047–1053.

Bell JC, Raynes-Greenow C, Bower C, et al. (2013) Descriptive epidemiology of cleft lip and cleft palate in Western Australia. *Birth Defects Res A Clin Mol Teratol* **97**, 101–108.

Bollert JA, Hendrickx AG (1971) Morphogenesis of the palate in the baboon (*Papio cynocephalus*). *Teratology* **4**, 343–354.

Braybrook C, Doudney K, Marcano AC, et al. (2001) The T-box transcription factor gene TBX22 is mutated in X-linked cleft palate and ankyloglossia. *Nat Genet* **29**, 179–183.

Breckpot J, Anderlid BM, Alanay Y, et al. (2015) Chromosome 22q12.1 microdeletions: confirmation of the MN1 gene as a candidate gene for cleft palate. *Eur J Hum Genet* doi: 10.1038/ejhg.2015.65

Burdi AR, Faist K (1967) Morphogenesis of palate in normal human embryos with special emphasis on mechanisms involved. *Am J Anat* **120**, 149–160.

Bush JO, Jiang R (2012) Palatogenesis: morphogenetic and molecular mechanisms of secondary palate development. *Development* **139**, 231–243.

Calnan J (1954) Submucous cleft palate. *Br J Plast Surg* **6**, 264–282.

Cardoso S, Robertson SP, Daniel PB (2012) *TGFBR1* mutations associated with Loeys-Dietz syndrome are inactivating. *J Recept Signal Transduct Res* **32**, 150–155.

Caylakli F, Yavuz H, Bolat F, et al. (2005) Epithelial cyst of the soft palate. *Int J Pediatr Otorhinolaryngol* **69**, 545–547.

Coleman RD (1965) Development of the rat palate. *Anat Rec* **151**, 107–117.

Cox TC (2004) Taking it to the max: the genetic and developmental mechanisms coordinating midfacial morphogenesis and dysmorphology. *Clin Genet* **65**, 163–176.

Creuzet S, Couly G, Le Douarin NM (2005) Patterning the neural crest derivatives during development of the vertebrate head: insights from avian studies. *J Anat* **207**, 447–459.

Cuervo R, Covarrubias L (2004) Death is the major fate of medial edge epithelial cells and the cause of basal lamina degradation during palatogenesis. *Development* **131**, 15–24.

Cuervo R, Valencia C, Chandraratna RA, et al. (2002) Programmed cell death is required for palate shelf fusion and is regulated by retinoic acid. *Dev Biol* **245**, 145–156.

Cui XM, Chai Y, Chen J, et al. (2003) TGF-β3-dependent SMAD2 phosphorylation and inhibition of MEE proliferation during palatal fusion. *Dev Dyn* **227**, 387–394.

Cui XM, Shiomi N, Chen J, et al. (2005) Overexpression of Smad2 in Tgf-β3-null mutant mice rescues cleft palate. *Dev Biol* **278**, 193–202.

Davidson TB, Sanchez-Lara PA, Randolph LM, et al. (2012) Microdeletion del(22) (q12.2) encompassing the facial development-associated gene, MN1 (meningioma 1) in a child with Pierre-Robin sequence (including cleft palate) and neurofibromatosis 2 (NF2): a case report and review of the literature. *BMC Med Genet* **13**, 19.

De la Cuadra Blanco C, Peces Pena MD, Rodriguez-Vazquez JF, et al. (2012) Development of the human tensor veli palatini: specimens measuring 13.6–137 mm greatest length; weeks 6–16 of development. *Cells Tissues Organs* **195**, 392–399.

DeAngelis V, Nalbandian J (1968) Ultrastructure of mouse and rat palatal processes prior to and during secondary palate formation. *Arch Oral Biol* **13**, 601–608.

Diewert VM (1983) A morphometric analysis of craniofacial growth and changes in spatial relations during secondary palatal development in human embryos and fetuses. *Am J Anat* **167**, 495–522.

Diewert VM (1985) Development of human craniofacial morphology during the late embryonic and early fetal periods. *Am J Orthod* **88**, 64–76.

Diewert VM (1986) Craniofacial growth during human secondary palate formation and potential relevance of experi-

mental cleft palate observations. *J Craniofac Genet Dev Biol Suppl* **2**, 267–276.

Diewert VM, Shiota K (1990) Morphological observations in normal primary palate and cleft lip embryos in the Kyoto collection. *Teratology* **41**, 663–677.

Dixon MJ, Marazita ML, Beaty TH, et al. (2011) Cleft lip and palate: understanding genetic and environmental influences. *Nat Rev Genet* **12**, 167–178.

Dudas M, Nagy A, Laping NJ, et al. (2004) Tgf-β3-induced palatal fusion is mediated by Alk-5/Smad pathway. *Dev Biol* **266**, 96–108.

Ferguson MW (1981) The structure and development of the palate in *Alligator mississippiensis*. *Arch Oral Biol* **26**, 427–443.

Fitchett JE, Hay ED (1989) Medial edge epithelium transforms to mesenchyme after embryonic palatal shelves fuse. *Dev Biol* **131**, 455–474.

Funato N, Nakamura M, Richardson JA, et al. (2012) Tbx1 regulates oral epithelial adhesion and palatal development. *Hum Mol Genet* **21**, 2524–2537.

Gosain AK, Conley SF, Santoro TD, et al. (1999) A prospective evaluation of the prevalence of submucous cleft palate in patients with isolated cleft lip versus controls. *Plast Reconstr Surg* **103**, 1857–1863.

Gritli-Linde A (2007) Molecular control of secondary palate development. *Dev Biol* **301**, 309–326.

Gu S, Wei N, Yu X, et al. (2008) Mice with an anterior cleft of the palate survive neonatal lethality. *Dev Dyn* **237**, 1509–1516.

Ha KM, Cleland H, Greensmith A, et al. (2013) Submucous cleft palate: an often-missed diagnosis. *J Craniofac Surg* **24**, 878–885.

Hilliard SA, Yu L, Gu S, et al. (2005) Regional regulation of palatal growth and patterning along the anterior-posterior axis in mice. *J Anat* **207**, 655–667.

Humphrey T (1969) The relation between human fetal mouth opening reflexes and closure of the palate. *Am J Anat* **125**, 317–344.

Iwata J, Suzuki A, Pelikan RC, et al. (2013) *Smad4-Irf6* genetic interaction and TGFβ-mediated IRF6 signaling cascade are crucial for palatal fusion in mice. *Development* **140**, 1220–1230.

Iwata J, Suzuki A, Yokota T, et al. (2014) TGFβ regulates epithelial-mesenchymal interactions through WNT signaling activity to control muscle development in the soft palate. *Development* **141**, 909–917.

Jerome LA, Papaioannou VE (2001) DiGeorge syndrome phenotype in mice mutant for the T-box gene, *Tbx1*. *Nat Genet* **27**, 286–291.

Jiang R, Bush JO, Lidral AC (2006) Development of the upper lip: morphogenetic and molecular mechanisms. *Dev Dyn* **235**, 1152–1166.

Jin JZ, Ding J (2006) Analysis of cell migration, transdifferentiation and apoptosis during mouse secondary palate fusion. *Development* **133**, 3341–3347.

Jugessur A, Farlie PG, Kilpatrick N (2009) The genetics of isolated orofacial clefts: from genotypes to subphenotypes. *Oral Dis* **15**, 437–453.

Kaartinen V, Voncken JW, Shuler C, et al. (1995) Abnormal lung development and cleft palate in mice lacking TGF-β3 indicates defects of epithelial-mesenchymal interaction. *Nat Genet* **11**, 415–421.

Kaartinen V, Cui XM, Heisterkamp N, et al. (1997) Transforming growth factor-β3 regulates transdifferentiation of medial edge epithelium during palatal fusion and associated degradation of the basement membrane. *Dev Dyn* **209**, 255–260.

Kara CO, Kara IG (2007) Persistent buccopharyngeal membrane. *Otolaryngol Head Neck Surg* **136**, 1021–1022.

Kitamura H (1966) Epithelial remnants and pearls in the secondary palate in the human abortus: a contribution to the study of the mechanism of cleft palate formation. *Cleft Palate J* **3**, 240–257.

Kitamura H (1989) *Embryology of the Mouth and Related Structures*. Tokyo: Maruzen Co. Ltd.

Kummer AW, Marshall JL, Wilson MM (2015) Non-cleft causes of velopharyngeal dysfunction: implications for treatment. *Int J Pediatr Otorhinolaryngol* **79**, 286–295.

Leslie EJ, Marazita ML (2013) Genetics of cleft lip and cleft palate. *Am J Med Genet C Semin Med Genet* **163C**, 246–258.

Lewin ML, Croft CB, Shprintzen RJ (1980) Velopharyngeal insufficiency due to hypoplasia of the musculus uvulae and occult submucous cleft palate. *Plast Reconstr Surg* **65**, 585–591.

Liu W, Lan Y, Pauws E, et al. (2008) The Mn1 transcription factor acts upstream of *Tbx22* and preferentially regulates posterior palate growth in mice. *Development* **135**, 3959–3968.

Loeys BL, Chen J, Neptune ER, et al. (2005) A syndrome of altered cardiovascular, craniofacial, neurocognitive and skeletal development caused by mutations in TGFBR1 or TGFBR2. *Nat Genet* **37**, 275–281.

Lowry RB (1970) Sex-linked cleft palate in a British Columbia Indian family. *Pediatrics* **46**, 123–128.

Lowry RB (1971) X-linked cleft palate. *Birth Defects Orig Artic Ser* **7**, 76–79.

Marcano AC, Doudney K, Braybrook C, et al. (2004) *TBX22* mutations are a frequent cause of cleft palate. *J Med Genet* **41**, 68–74.

Martinez-Alvarez C, Tudela C, Perez-Miguelsanz J, et al. (2000) Medial edge epithelial cell fate during palatal fusion. *Dev Biol* **220**, 343–357.

Meester-Smoor MA, Vermeij M, van Helmond MJ, et al. (2005) Targeted disruption of the Mn1 oncogene results in severe defects in development of membranous bones of the cranial skeleton. *Mol Cell Biol* **25**, 4229–4236.

Miettinen PJ, Chin JR, Shum L, et al. (1999) Epidermal growth factor receptor function is necessary for normal craniofacial development and palate closure. *Nat Genet* **22**, 69–73.

Mogass M, Bringas P Jr, Shuler CF (2000) Characterization of desmosomal component expression during palatogenesis. *Int J Dev Biol* **44**, 317–322.

Monteagudo B, Labandeira J, Cabanillas M, et al. (2012) Prevalence of milia and palatal and gingival cysts in Spanish newborns. *Pediatr Dermatol* **29**, 301–305.

Mossey PA, Castilla EE (2003) *Global Registry and Database on Craniofacial Anomalies*. Geneva: World Health Organization.

Mossey PA, Little J, Munger RG, et al. (2009) Cleft lip and palate. *Lancet* **374**, 1773–1785.

Nakajima A, Ito Y, Asano M, et al. (2007) Functional role of transforming growth factor-β type III receptor during palatal fusion. *Dev Dyn* **236**, 791–801.

Nawshad A (2008) Palatal seam disintegration: to die or not to die? That is no longer the question. *Dev Dyn* **237**, 2643–2656.

Ooë T (1981) *Human Tooth and Dental Arch Development*. Tokyo: Ishiyaku Publishers Inc.

O'Rahilly R, Muller F (2001) *Human Embryology and Teratology*. New York: Wiley-Liss.

Papangeli I, Scambler P (2013) The 22q11 deletion: DiGeorge and velocardiofacial syndromes and the role of TBX1. *Wiley Interdiscip Rev Dev Biol* **2**, 393–403.

Pauws E, Hoshino A, Bentley L, et al. (2009) *Tbx22null* mice have a submucous cleft palate due to reduced palatal bone formation and also display ankyloglossia and choanal atresia phenotypes. *Hum Mol Genet* **18**, 4171–4179.

Poswillo D (1974) The pathogenesis of submucous cleft palate. *Scand J Plastic Recon Surg* **8**, 34–41.

Presland RB, Dale BA (2000) Epithelial structural proteins of the skin and oral cavity: function in health and disease. *Crit Rev Oral Biol Med* **11**, 383–408.

Proetzel G, Pawlowski SA, Wiles MV, et al. (1995) Transforming growth factor-β 3 is required for secondary palate fusion. *Nat Genet* **11**, 409–414.

Pruzansky S (1961) *Congenital Anomalies of the Face and Associated Structures*. Springfield: Charles C Thomas.

Rood SR (1973) The morphology of *M. tensor* veli palatini in the five-month human fetus. *Am J Anat* **138**, 191–195.

Ruda JM, Krakovitz P, Rose AS (2012) A review of the evaluation and management of velopharyngeal insufficiency in children. *Otolaryngol Clin North Am* **45**, 653–669, viii.

Saunders ID (1972) Bohn's nodules. A case report. *Br Dent J* **132**, 457–458.

Schupbach PM (1983) Experimental induction of an incomplete hard-palate cleft in the rat. *Oral Surg Oral Med Oral Pathol* **55**, 2–9.

Shaw RM, Chaudry AP (1974) Light microscopic and histochemical observations on the development of the palate in the Golden Syrian hamster. *J Anat* **117**, 1–15.

Shprintzen RJ, Schwartz RH, Daniller A, et al. (1985a) Morphologic significance of bifid uvula. *Pediatrics* **75**, 553–561.

Shprintzen RJ, Siegel-Sadewitz VL, Amato J, et al. (1985b) Anomalies associated with cleft lip, cleft palate, or both. *Am J Med Genet* **20**, 585–595.

Smiley GR (1975) A histological study of the formation and development of the soft palate in mice and man. *Arch Oral Biol* **20**, 297–298.

Smiley GR, Koch WE (1972) An *in vitro* and *in vivo* study of single palatal processes. *Anat Rec* **173**, 405–415.

Smith TM, Lozanoff S, Iyyanar PP, et al. (2012) Molecular signaling along the anterior-posterior axis of early palate development. *Front Physiol* **3**, 488.

Sperber GH, Guttman GD (2010) *Craniofacial Embryogenetics and Development*. Shelton, CT: People's Medical Pub. House USA.

Suphapeetiporn K, Tongkobpetch S, Siriwan P, et al. (2007) *TBX22* mutations are a frequent cause of non-syndromic cleft palate in the Thai population. *Clin Genet* **72**, 478–483.

Suzuki S, Marazita ML, Cooper ME, et al. (2009) Mutations in BMP4 are associated with subepithelial, microform, and overt cleft lip. *Am J Hum Genet* **84**, 406–411.

Tsai WC, Kuo CY, Wang CH (2013) Epidermal inclusion cyst of the soft palate and uvula in an infant. *Eur J Pediatr* **172**, 1563–1564.

Van Laer L, Dietz H, Loeys B (2014) Loeys-Dietz syndrome. *Adv Exp Med Biol* **802**, 95–105.

Verma SP, Geller K (2009) Persistent buccopharyngeal membrane: report of a case and review of the literature. *Int J Pediatr Otorhinolaryngol* **73**, 877–880.

Walker BE, Fraser FC (1956) Closure of the secondary palate in 3 strains of mice. *J Embryol Exp Morphol* **4**, 176–189.

Waterman RE (1977) Ultrastructure of oral (buccopharyngeal) membrane formation and rupture in the hamster embryo. *Dev Biol* **58**, 219–229.

Weatherley-White RC, Sakura CY Jr, Brenner LD, et al. (1972) Submucous cleft palate. Its incidence, natural history, and indications for treatment. *Plast Recon Surg* **49**, 297–304.

Wood PJ, Kraus BS (1962) Prenatal development of the human palate. Some histological observations. *Arch Oral Biol* **7**, 137–150.

Wyszynski DF (2002) *Cleft Lip and Palate: from Origin to Treatment*. Oxford: Oxford University Press.

Xu X, Han J, Ito Y, et al. (2006) Cell autonomous requirement for *Tgfbr2* in the disappearance of medial edge epithelium during palatal fusion. *Dev Biol* **297**, 238–248.

Yu L, Gu S, Alappat S, et al. (2005) *Shox2*-deficient mice exhibit a rare type of incomplete clefting of the secondary palate. *Development* **132**, 4397–4406.

Supporting Information

Additional Supporting Information may be found in the online version of this article:

Fig. S1. Staging criteria used by University of Washington included crown rump length (CRL) and foot length.

Fig. S2. A 54-day specimen stained with H & E with a partially fused anterior soft palate.

Fig. S3. A 57-day specimen stained with H & E demonstrating a seam throughout the soft palate.

Fig. S4. A 67-day specimen sectioned through the soft palate.

Fig. S5. A 70-day specimen with a fully fused hard and soft palate.